

Contribution from the Laboratoire de Chimie des Solides,
U.E.R. de Chimie, Université de Nantes, 44072-Nantes Cédex, France

Physical Properties of Lithium Intercalation Compounds of the Layered Transition Chalcogenophosphates

R. BREC, D. M. SCHLEICH,* G. OUVARD, A. LOUISY, and J. ROUXEL

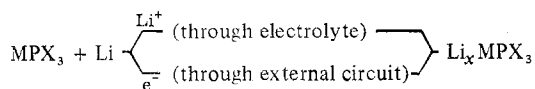
Received September 15, 1978

The layered transition chalcogenophosphates MPX_3 have recently been shown to function as cathodes in lithium batteries. In this study, we have prepared several members of the series MPX_3 ($M = Fe, Ni, Mn; X = S, Se$) in order to observe their physical properties and the effects on these physical properties of chemical intercalation with *n*-butyllithium. Optical studies have shown that compounds that have a low energy gap behave as good cathode materials: this is the case of $FePS_3$, $NiPS_3$, and $FePS_3$. For materials with a high energy gap (>2.5 eV) no intercalation is observed. Magnetic studies show no change in the antiferromagnetic characteristics of $FePS_3$, $FePSe_3$, and $MnPSe_3$ after intercalation. However, a decrease of magnetic susceptibility observed in Li_xNiPS_3 can be explained through the occurrence of multiple phase domains. Optical and conductivity measurements show that intercalations result in the occurrence of negative free carriers that seem to correspond to metallike behavior in the case of Li_xNiPS_3 .

Introduction

It has been shown recently^{1,2} that layered MPX_3 reacts chemically with *n*-butyllithium or electrochemically with lithium to give intercalated products. These thio- or seleniophosphates, which may be viewed as the substitution of one-third of the metal by P_2 groups in a MX_2 formula ($M_{2/3}(P_2)_{1/3}X_2$),³ exhibit a van der Waals gap between the $[XM_{2/3}(P_2)_{1/3}X]$ slabs (Figures 1 and 2). Whereas lithium intercalation in the transition-metal dichalcogenides is followed by parameter expansion, the MPX_3 intercalation does not result in any noticeable change in the X-ray spectra. This makes it difficult to determine the limit of chemical intercalations. However, electrochemical studies near thermodynamic equilibrium conditions have indicated a limit close to 1.5 lithium atoms/ $NiPS_3$.² This limit would correspond to a total occupancy of the octahedral sites in the gap of the MPX_3 phases and would be in agreement with what is observed in the lithium intercalates of layered MX_2 with the Li_1MX_2 limit.^{4,5}

Among the chalcogenophosphates that have been tested, only $NiPS_3$, $FePSe_3$, and, to a lesser degree, $FePS_3$ have behaved as good cathode materials. The reaction



takes place in a battery: Li/propylene carbonate (1 M $LiClO_4$ /pressed MPX_3). In order to understand the differences existing among the members of the MPX_3 group, we have performed physical measurements on some starting compounds and their lithium intercalated products. We report here the magnetic, optical, and conductivity measurements of Li_xNiPS_3 , Li_xFePSe_3 , and Li_xFePS_3 . The results obtained are compared and discussed with those gathered for poor cathode materials such as $MnPSe_3$ and $MnPSe_3$.

Experimental Section

All the MPX_3 compounds were prepared from the elements, by using previously reported conditions.^{3,6-8} The selenide derivatives were handled in dry atmosphere as they react with air moisture; for example, after several days in air, pure $FePSe_3$ was found to present some ferromagnetic impurities.

X-ray analysis was performed by using $Cu K\alpha$ radiation, with either a diffractometer or a Debye-Scherrer chamber with a nominal diameter of 114.83 mm. For hygroscopic intercalates, capillary tubes were filled with the powder in a drybox and sealed under vacuum.

Due to previously reported nonstoichiometry in $FePS_3$,¹ density measurements were made on single crystals by using the buoyancy

principle with CCl_4 as the liquid. The sample showed an experimental density of $d = 3.10 \pm 0.3$ g cm^{-3} within the error limits of the theoretical density (3.09 g cm^{-3}).

All intercalation reactions between MPX_3 compounds and *n*-butyllithium solution in hexane were carried out in a dry, oxygen-free atmosphere. Previous studies have frequently used temperatures ranging from 68 (hexane boiling point) to 60 °C⁵ to chemically intercalate lithium in layered compounds with *n*-butyllithium. However, we observed² after several days of reaction between MPX_3 and *n*-butyllithium at 68 °C, the occurrence of Li_2S when reaching the composition 1.2 Li and 1.0 Li, respectively, for $NiPS_3$ and $FePS_3$. In the same experimental conditions Li_2Se was found in $Li_{1.0}FePSe_3$ and $Li_{1.25}MnPSe_3$. In addition, in the case of iron derivatives, experiments conducted in the above conditions showed ferromagnetic impurities. These experiments underline the poor stability of the Li_xMPX_3 phases and lead us to choose to intercalate lithium at 20 °C. *n*-Butyllithium in solution in hexane was left over ground powder of the material to be intercalated for 10–15 days at room temperature. After filtering and washing of the intercalated powders, lithium present in the filtered solution and in the dried powder was analyzed by flame spectroscopy. We systematically checked that the intercalated phases prepared did not contain any ferromagnetic impurity and the X-ray analysis always showed only the MPX_3 spectra of the studied starting material.

Magnetic susceptibility measurements were performed on polycrystalline samples by using the Faraday technique. The $H(\partial H/\partial z)$ values were calculated for various field strengths by using a platinum standard. A constant field strength of 7.4 kG was used for temperature-dependent measurements. The temperature was determined by using either a platinum resistor or a chromel–alumel thermocouple placed close to the sample. Hygroscopic intercalates were placed in a Teflon sample boat sealed with a tightly screwed Teflon cap. The nonintercalated samples were examined either in the same Teflon container or in a small quartz bucket.

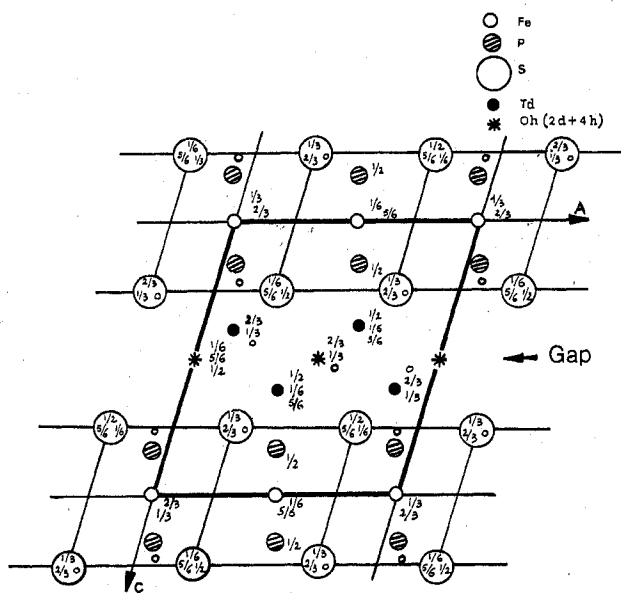
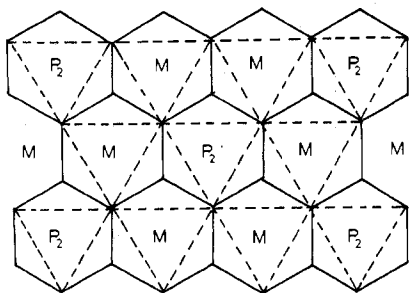
Optical absorption measurements were performed from 33,000 to 4,000 Å by using a Beckman DK 29 spectrophotometer. Thin samples were obtained by cleavage parallel to the close packing layers (i.e., perpendicular to the *c* axis in rhombohedral symmetry). Sample thicknesses were determined from microscope measurements and compared with the thicknesses calculated from interference fringes. Hygroscopic intercalated compounds were placed in sealed quartz cells under dry nitrogen before measurement.

Large single crystals were used for four-probe direct current electrical conductivity measurements, perpendicular to the *c* axis. Electrical contacts were made with indium ultrasonically soldered to the crystal. For measurements performed in the process and after intercalation, the crystals were placed in a sealed Pyrex tube with Pyrex-shielded platinum wires directly soldered to indium contacts. Additional contacts were available to verify that no substantial Faradic current flow occurred in the butyllithium/hexane solution during crystal measurements.

Results and Discussions

Crystallographic Results. Powders of $MnPSe_3$, $FePS_3$, $FePSe_3$, and $NiPS_3$ when placed in contact with *n*-butyllithium

* To whom correspondence should be addressed at the Laboratoire de Physique de la Matière Condensée Ecole Polytechnique, 91128 Palaiseau Cédex, France.

Figure 1. Structure of MPS_3 ($C2/m$).Figure 2. Metal (M) and phosphorus pairs (P_2) in sulfur polyhedra of a MPS_3 compound.

solutions in hexane at 25 °C show intercalation, whereas MnPS_3 (like CdPS_3 and ZnPS_3) shows almost no reaction.

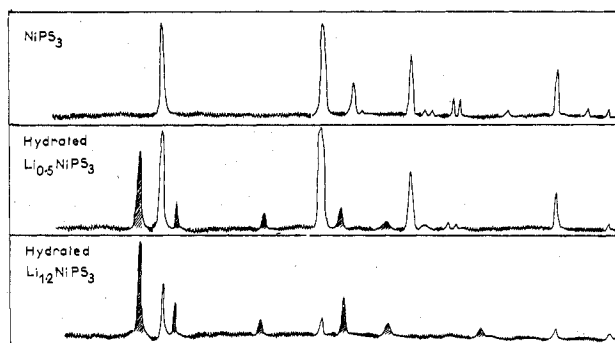
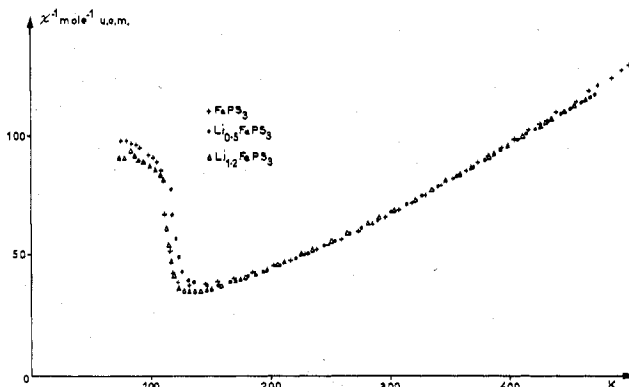
The following reaction accounts for the intercalation of lithium:



Maximum lithium uptake varies substantially with the concentration of *n*-butyllithium, and, as the X-ray spectra showed no change in the relative line intensities and positions, it has not been possible to determine a limit of intercalation. However, for high lithium uptake, it seems that the intensity of the spectra decreases. In particular, for the nickel derivatives, we observed a totally amorphous system for $\text{Li}_{3.6}\text{NiPS}_3$.

In the absence of any spectral modifications, it was not possible to explain, from X-ray analysis, the intercalation process. It could be either through gradual lithium diffusion in the MPX_3 structure with a nonstoichiometric Li_xMPX_3 phase becoming progressively enriched in lithium or through steps by the occurrence of stoichiometric $\text{Li}_{0.5}\text{NiPS}_3$ and $\text{Li}_{1.5}\text{NiPS}_3$ phases, as might be interpreted from our previous thermodynamic discharge curves.²

On contact with air moisture, the NiPS_3 intercalates undergo spontaneous hydration as can be seen on the X-ray spectra. This reaction is the first X-ray spectrographic indication of lithium intercalation in an MPX_3 host structure. As an example, Figure 3 shows that the line intensities of $\text{Li}_{0.5}\text{NiPS}_3$ decrease drastically giving rise to new spectra that show mostly 001 intense reflections corresponding to a Δc increase of 5.8 Å, consistent with the presence of two layers of water around lithium in the van der Waals gap.⁹ In analogous experiments carried out on $\text{Li}_{1.2}\text{NiPS}_3$ (Figure 3),

Figure 3. X-ray powder spectra of hydrated Li_xNiPS_3 .Figure 4. Inverse susceptibility of Li_xFePS_3 ($x = 0, 0.5, \text{ and } 1.2$) vs. T .Table I. Magnetic Data for Li_xMnPS_3 , Li_xFePS_3 , Li_xFePS_3 , and Li_xNiPS_3 ^a

composition	μ_{eff}, μ_B	Θ, K	T_N, K
MnPS_3	6.1	-201	85
$\text{Li}_{0.2}\text{MnPS}_3$	6.2	-201	87
$\text{Li}_{0.5}\text{MnPS}_3$	6.1	-194	83
Li_1MnPS_3	6.0	-190	85
FePS_3	5.0 (5.1)	-4 (37)	118 (123)
$\text{Li}_{0.44}\text{FePS}_3$	4.9	4	123
$\text{Li}_{0.74}\text{FePS}_3$	4.9	1	118
FePS_3	5.0 (5.4)	65 (14)	133 (126)
$\text{Li}_{0.5}\text{FePS}_3$	5.2	81	153
$\text{Li}_{1.2}\text{FePS}_3$	5.1	92	135
NiPS_3	3.9 (3.7)	-712 (-558)	300 (254)

^a Values in parentheses are from ref 10 and 11.

hydrated phases show the spectra of NiPS_3 much less intense. This tends to indicate that, in the $0 < x < 1.5$ interval, chemically intercalated Li_xNiPS_3 corresponds to a multiple phase system. This is consistent with the physical results (see below) that tend to show lithium intercalation takes place through a non-single-phase system.

Magnetic Measurements. Magnetic susceptibility data were collected for antiferromagnetic NiPS_3 , FePS_3 , and FeSe_3 . Least-squares fits were made for the plots of $1/\chi$ (molar corrected) vs. temperature (χ (molar corrected) = χ (molar) + χ (diamagnetic)) in the paramagnetic region to calculate the Curie constants. In Table I are listed the magnetic parameters we have observed in comparison with previously reported results.^{10,11} We calculated moments of 3.9 and 5.0 for NiPS_3 and FePS_3 calculated respectively in the 500–670 K and 250–400 K range. These moments are in good agreement with the published values of 3.7 and 5.1. However, for FePS_3 our calculated μ_{eff} of 5.0 μ_B is somewhat lower than the previously determined 5.4 μ_B . Our calculated μ_{eff} was obtained from data collected between 300 and 500 K as opposed to the previous work where the constant was calculated below 300 K. In the temperature range below 300 K, we

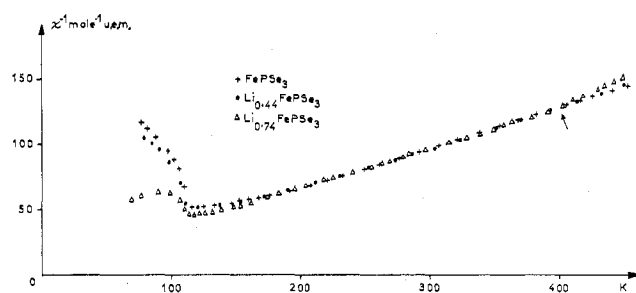


Figure 5. Inverse susceptibility of $\text{Li}_x\text{FePSe}_3$ ($x = 0, 0.44,$ and 0.74) vs. T . The arrow indicates irreversible decomposition temperature for $\text{Li}_{0.74}\text{FePSe}_3$ (Δ).

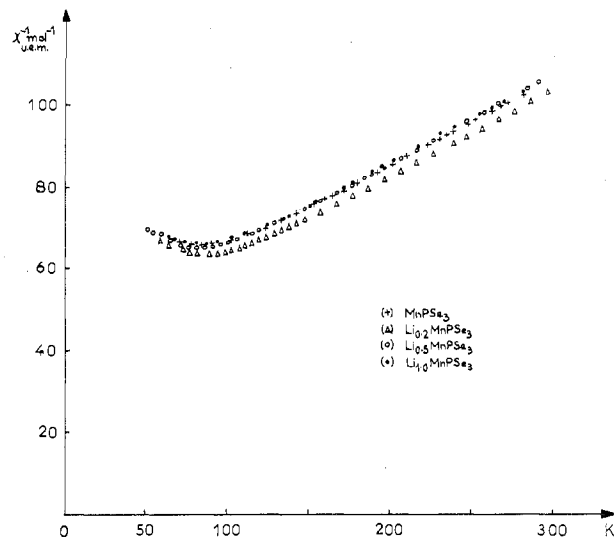


Figure 6. Inverse susceptibility of $\text{Li}_x\text{MnPSe}_3$ ($x = 0, 0.2, 0.5,$ and 1.0) vs. T .

observed a slight deviation from Curie-Weiss behavior with the Curie constant increasing as one approaches the Néel point (Figure 4).

MnPSe_3 was examined over the temperature range from 77 to 400 K (Figure 6). The compound showed susceptibility behavior indicative of antiferromagnetism. The moment was calculated between 150 and 400 K and led to μ_{eff} of $6.1 \mu_B$. This observed moment as well as the observed moments for the other MPX_3 compounds is readily explained by the existence of a localized $2+$ transition-metal ion. In the cases of Fe^{2+} and Mn^{2+} , the observed moments are in good agreement with a spin-only calculated moment $\mu_{\text{eff}} = [4S(S+1)]^{1/2}$; however, in the case of Ni^{2+} the observed moment is somewhat higher as would be expected, due to some spin-orbit coupling in addition to curve perturbations from the high-temperature Néel point.

Powder samples were intercalated by using the previously described butyllithium technique. Figures 4, 5, and 6 show curves of $1/\chi$ (molar corrected) vs. temperature for several Li intercalated compositions. As can be seen, we observed no noticeable changes in the susceptibility, observed moments, or Néel points for FePS_3 , FePSe_3 , or MnPSe_3 (Table I). The data collected for Li_xNiPS_3 (Figure 7) showed rather anomalous behavior. The μ_{eff} for the lithium intercalated species could not be reliably calculated since the materials showed a nonreversible decomposition at temperatures greater than 350 K (decomposition point is shown by arrows on the figure). However, the molar susceptibility decreased as the concentration of Li was increased with a Néel point which remained rather constant. This result seems to coincide with the X-ray diffraction studies performed on hydrated Li_xNiPS_3 compositions indicating a two-phase domain. This two-phase

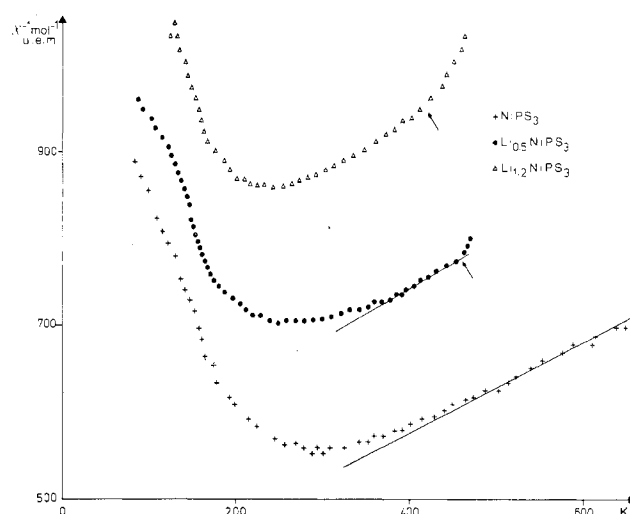


Figure 7. Inverse susceptibility of Li_xNiPS_3 ($x = 0, 0.5,$ and 1.2) vs. T . The arrows indicate irreversible decomposition temperature.

Table II. Resistivity Measurements Obtained during Lithium Intercalation in FePS_3 and NiPS_3

T	$R, \Omega \text{ cm}$
FePS_3 (15% <i>n</i>-Butyllithium Solution)	
0 ^a	2.5×10^4
1 h	1.16×10^3
24 h	1.03×10^3
48 h	3.54×10
120 h	2.95×10^b
NiPS_3 (0.1% <i>n</i>-Butyllithium Solution)	
0	10^9
5 min	9×10^3
15 min	6.1×10
60 min	1.84×10

^a Before intercalation. ^b $\text{Li}_{0.3}\text{FePS}_3$.

domain appears to be composed of a temperature-dependent magnetic phase and a second phase with a substantially reduced susceptibility.

Conductivity. Four-probe Van der Pauw conductivity measurements have been performed on various crystals of FePS_3 , FePSe_3 , NiPS_3 , and MnPSe_3 . Voltages were determined by using a Keithley high-impedance electrometer and the ohmicity of all measurements was checked by varying the current from 0.1 to 1000 μA where possible. The crystals of NiPS_3 and MnPSe_3 had extremely high resistances $\sim 10^9 \Omega \text{ cm}$ which presented impedance problems therefore preventing accurate determination before intercalation. Single crystals of FePS_3 and FePSe_3 on the other hand had values of between 10^4 and $10^5 \Omega \text{ cm}$, with slight variation from crystal to crystal. Room-temperature Seebeck measurements indicated positive type carriers for FePS_3 and FePSe_3 . The reduced resistivity for the iron compounds is consistent with a slight nonstoichiometry which has been previously observed for FePS_3 .¹

Several crystals of the above compounds were placed in contact with butyllithium/hexane solutions of varying concentrations, and the evolution of conductivity was monitored as a function of time. No change has been observed in the conductivity of MnPSe_3 even when left in contact with 15% BuLi /hexane for periods up to 10 days. Crystals of FePS_3 and FePSe_3 showed a gradual and continuous decrease in resistivity which depended on the concentration of the butyllithium-hexane solution as well as the contact time. Table II shows a typical result obtained for a crystal of FePS_3 which was placed in contact with a butyllithium/hexane solution. After the fifth day of contact, the hexane/butyllithium solution was removed and the sample was cooled to liquid-nitrogen temperatures. For the particular example cited in Table II,

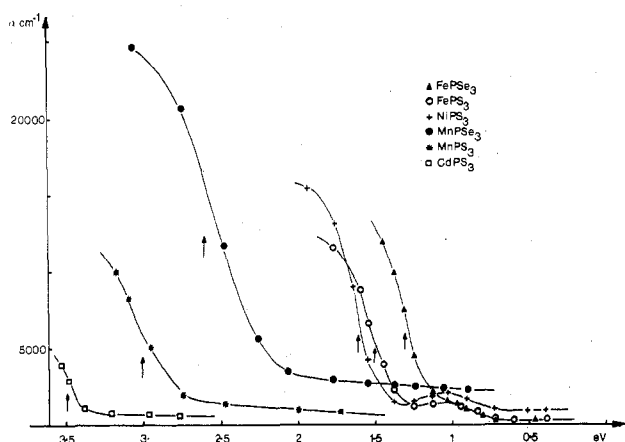


Figure 8. Arrows indicate a break in the absorption curve and correspond to the energy gap.

the resistivity ratio R_{77}/R_{300} was 40. This particular sample was analyzed for lithium content by flame spectroscopy and was found to have 0.3 mol of lithium/mol of FePS_3 . For all samples of FePS_3 and FePSe_3 , the change in resistivity was gradual even when the concentration of the solution was increased to 15% in butyllithium. Room-temperature Seebeck measurements indicated that after the intercalation process the compositions showed n-type conductivity and R_{77}/R_{300} resistivity ratios of approximately 2 orders of magnitude.

In the case of NiPS_3 we have observed a large and rapid decrease of resistivity in all cases. Even when the butyllithium concentration was reduced to less than 1% (Table II), after 1 h, samples showed resistivities of approximately $10 \Omega \text{ cm}$. After contact for longer periods of time the resistivity continued to decrease; however, stable readings were usually obtained after 1 or 2 days with values at room temperature of $\sim 10^{-2} \Omega \text{ cm}$. Analysis of a crystal after several hours of contact with a resistivity of approximately $1 \Omega \text{ cm}$ yielded an overall lithium content of 0.2 mol of Li/mol of NiPS_3 . After the cooling of NiPS_3 samples to liquid-nitrogen temperature, resistivity ratios R_{77}/R_{300} between 1 and 2 were observed.

The electrical behavior of the MPX_3 compounds appears as three general categories: the MnPSe_3 where one does not observe an increase in the conductivity (therefore the number of electrical carriers remains very low), the iron group where one observes a gradual increase in the number of carriers which appear to be thermally activated, and NiPS_3 where the number of carriers increases rapidly and do not appear to be thermally activated.

In the case of MnPSe_3 , two explanations may be put forth to explain the high resistivity value: (1) The possibility exists that the rate of intercalation at room temperature of a single crystal is so slow that after 2 days no appreciable reaction is observed. (2) The electrons arising from an ionization of lithium remain trapped in a deep lying state and, at room temperature, are not activated to the conduction band. For FePS_3 , FePSe_3 , and NiPS_3 , conduction electrons are introduced by intercalation with butyllithium. In FePS_3 and FePSe_3 , these electrons appear to be in a level lying close to the conduction band, whereas in NiPS_3 the donated electrons might well enter directly into the conduction band. However, without Hall effect data to determine if there are changes in the mobility, the resistivity data alone is not a definitive proof of thermal activation.

Optical Measurements. Optical absorption measurements have been performed on single crystals of NiPS_3 , FePS_3 , FePSe_3 , MnPS_3 , MnPSe_3 , and CdPS_3 . Figure 8 shows the curves of the absorption coefficient α vs. energy (eV) for this series. In most of these compounds, there are rather intense d-d transitions which occur at values close to the fundamental

MnPS_3^* 3.0 eV	FePS_3^* 1.5 eV	NiPS_3^* 1.6 eV	ZnPS_3^* 3.4 eV	
MnPSe_3^* 2.5 eV	FePSe_3^* 1.3 eV		CdPS_3^* 3.5 eV	$\text{In}_{2/3}\text{PS}_3$ 3.1 eV
				$\text{In}_{2/3}\text{PSe}_3$ 1.9 eV

Figure 9. Absorption edge of some MPX_3 phases. Asterisk indicates this work.

absorption and make intensity calculations rather difficult. The arrows on Figure 8 indicating the energy gaps are at those positions where one observes a break in the curve. All members in this series are broad band semiconductors with gap values ranging from 1.3 eV for FePSe_3 to 3.5 eV for CdPS_3 (Figure 9). As would be expected, a given selenide presents a smaller energy gap than the corresponding sulfide. It is worth noting that the three materials NiPS_3 , FePS_3 , and FePSe_3 which have proved to be the best cathodes² appear to have energy gaps substantially lower than the materials which do not intercalate or intercalate poorly. These three materials are also the same which have shown large decreases in conductivity during intercalation. One might view this from a simple band model where the process of Li intercalation is energetically favorable only in those cases where an unoccupied band is at an energy sufficiently low to readily accommodate an additional electron. Optical transmission measurements were also attempted after intercalation; however, several problems were encountered. In samples of NiPS_3 , no transmittance of light was observed in the spectral range from 33 000 to 5000 Å. Also, due to the speed of this reaction, attempts to follow this decrease in transmittance as a function of time were not successful. In the cases of FePS_3 and FePSe_3 , after slight intercalation, we did observe a decrease in transmission in the low-energy range before a total loss of transmission. In MnPSe_3 no change was observed in the transmission spectra after contact with butyllithium. These results are consistent with an increased electrical conductivity in NiPS_3 , FePS_3 , and FePSe_3 where the number of electrical carriers has drastically increased, resulting in free carrier absorption and increased reflectivity.

Conclusion

We have undertaken a study on a series of compounds with the general formula MPX_3 . The nature of this study was centered around the physical properties of the compounds with respect to their intercalates in order to better understand the process of intercalation.

We have observed that, although all the members in this series have available vacancies in the van der Waals gap, their ability to accommodate intercalated lithium is certainly not the same. In those materials with very large optical band gaps (i.e., MnPS_3 and CdPS_3) we have observed no chemical intercalation. In MnPSe_3 , chemical analysis has indicated that substantial quantities of lithium has entered the compound in powder. However, single crystals showed neither optical nor electrical change. If intercalation has occurred in the single crystals, it must be assumed that the electrons originating from ionized lithium atoms remain separated from the conduction band by an energy value greater than kT ($T = 300 \text{ K}$). In FePS_3 , FePSe_3 , and NiPS_3 , the physical properties have been substantially altered by this intercalation process. In the iron compounds, the system retains the same localized magnetic moment; however, the electrical conductivity decreases noticeably. This system shows a substantial increase in the

number of electrical carriers but these carriers do not appear to be free but rather close to the conduction band. In NiPS₃ the intercalation is more rapid and probably occurs as a two-phase phenomenon. The reduction in magnetic susceptibility as well as the large number of nonthermally activated electrons suggests the formation of a metallic intercalated phase. This argument is supported by recent NMR measurements which have observed a second phosphorus resonance peak with lithium intercalation.¹²

It is interesting to compare the results obtained by chemical intercalation with those previously reported for electrochemical discharge. For those materials which show no change in electrical conductivity with chemical intercalation the electrical discharge drops rapidly. NiPS₃ which is the material that chemically reacted the most rapidly and showed the largest change in electrical and magnetic properties has also shown the most favorable discharge curves. It must be emphasized that the chemical intercalations carried out with butyllithium were certainly not under thermodynamic equilibrium conditions and therefore would not necessarily yield the same results as those experiments made electrochemically.

Registry No. MnPSe₃, 69447-58-1; FePSe₃, 52226-00-3; FePS₃, 42821-47-6; NiPS₃, 42821-48-7; MnPS₃, 43000-56-2; CdPS₃, 60495-79-6; ZnPS₃, 56172-70-4; LiMnPSe₃, 70130-39-1; LiFePSe₃, 70130-40-4; LiFePS₃, 70130-41-5; LiNiPS₃, 65756-46-9; *n*-butyllithium, 109-72-8.

References and Notes

- (1) A. H. Thompson and M. S. Whittingham, *Mater. Res. Bull.*, **12**, 741 (1977).
- (2) A. Le Mehaute, G. Ouvrard, R. Brec, and J. Rouxel, *Mater. Res. Bull.*, **12**, 1191 (1977).
- (3) W. Klingen, Dissertation, Universität Hohenheim, Germany, 1969.
- (4) M. B. Dines, *Mater. Res. Bull.*, **10**, 287, 1975.
- (5) D. Murphy, F. Di Salvo, G. W. Hull, and J. Waszczak, *Inorg. Chem.*, **15**, 17 (1976).
- (6) W. Klingen, G. Eulenberger, and H. Hahn, *Naturwissenschaften*, **55**, 229 (1968).
- (7) W. Klingen, G. Eulenberger, and H. Hahn, *Naturwissenschaften*, **57**, 88 (1970).
- (8) R. Nitsche and P. Wild, *Mater. Res. Bull.*, **5**, 419 (1970).
- (9) A. Lerf and R. Schollhorn, *Inorg. Chem.*, **16**, 2950 (1977).
- (10) B. E. Taylor, J. Steger, and A. Wold, *J. Solid State Chem.*, **7**, 461 (1973).
- (11) B. E. Taylor, J. Steger, A. Wold, and E. Kostiner, *Inorg. Chem.*, **13**, 2719 (1974).
- (12) C. Berthier, Y. Chabre, and M. Minier, *Solid State Commun.*, **28**, 327 (1978).

Contribution from the Department of Chemistry,
Kansas State University, Manhattan, Kansas 66506

Quantum Yields and Product Stereochemistry for the Photochemistry of *cis*- and *trans*-Rh(en)₂XClⁿ⁺ 1

JOHN D. PETERSEN* and FRANK P. JAKSE

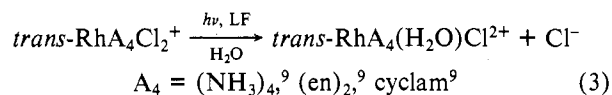
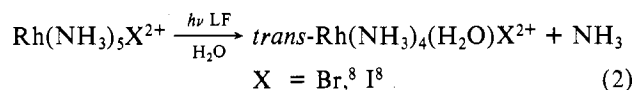
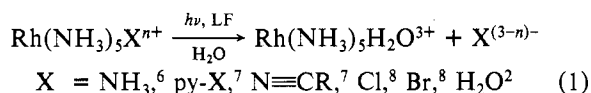
Received August 23, 1978

The photoaquation quantum yields and product stereochemistries for *cis*- and *trans*-Rh(en)₂XClⁿ⁺ (X = Cl, NH₃) are reported. All of the complexes undergo loss of chloro ligand and formation of Rh(en)₂X(H₂O)ⁿ⁺ in aqueous solution. Photolysis of the *trans* complexes results in stereoretentive products with quantum yields of 0.061 and 0.062 mol/einstein for X = Cl and NH₃, respectively. For the *cis* complexes, the stereochemistry of the product depends on the nature of X. For X = Cl, the quantum yield for chloro loss is 0.43 mol/einstein, and the product has a *trans* configuration. For X = NH₃, chloro loss ($\Phi = 0.145$ mol/einstein) results in the stereoretentive *cis* photoproduct. The stereochemical fate and mechanistic implications of the photolysis reactions of these Rh(III) amine complexes will be discussed in terms of existing theory.

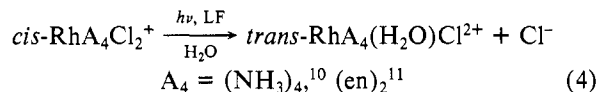
Introduction

Ligand field photolysis of rhodium(III) amine complexes in aqueous solution customarily leads to the photoaquation of one ligand from the complex² resulting in a monoquo complex as the photolysis product. Subsequent ligand photosubstitution reactions are not observed spectroscopically since further reaction is usually limited to aquo ligand exchange.³ Models⁴ have been proposed to explain the nature of the labilized ligand although some ambiguities⁵ arise in the correlation of theory to experiment.

Until recently, the theory on the photosubstitution reactions of rhodium(III) amine complexes has been limited to the nature of the labilized ligand with no effort spent on the stereochemistry of the remaining metal fragment. This apparent lack of study was manifested by the seemingly stereoretentive photochemical behavior of the Rh(III) complexes. Photolyses of pentaamminerhodium(III) systems (eq 1 and 2) and *trans*-disubstituted tetraamine complexes (eq 3) have



led solely to pentaammine or *trans*-disubstituted tetraamine photolysis products. It was not until studies on the photochemistry^{10,11} of *cis*-dichlorotetraamminerhodium(III) complexes resulted in *trans* products (eq 4) did any thermal¹²



or photochemical substitution reaction of Rh(III) definitely indicate geometric isomerization around the metal center.

Cis/trans rearrangements of M(III) amine complexes are not limited to Rh(III). Both Co(III)^{13,14} and Cr(III)¹⁵ amine complexes display stereomobility during photosubstitution reactions. Vanquickenborne and Ceulemans^{16,17} have been successful recently in using a ligand field treatment to explain the stereochemical changes around selected d³ and d⁶ metal centers.

In this work, we report the results of the ligand field photochemistry of some bis(ethylenediamine) complexes of Rh(III). In addition, we will use the ligand field analysis of Vanquickenborne and Ceulemans¹⁷ to discuss the stereochemistry of the photolysis products of these reactions as well